

TRANSPORT CALCULATIONS FOR GAMMA-RAY BY INVARIANT EMBEDDING METHOD

Akinao SHMIZU

The Wakasa Wan Energy Research Center
64-52-1 Nagatani, Tsuruga, Fukui 914-0192 Japan
ashimizu@werc.or.jp

ABSTRACT

The method of invariant embedding has been applied to transport calculations for gamma-ray with real cross sections depending upon energy and angle. Some problems including excessive amount of space meshes met in transport calculations for gamma-ray are discussed, followed by the features of the invariant embedding method developed to overcome these difficulties. The method is proved to be practically free from space mesh and can be applied to deep penetration problems. Some results of calculations for exposure buildup factors of gamma-ray up to depths as large as 300 mean free paths are presented.

1. INTRODUCTION

The present paper concerns transport calculations for gamma-ray by the invariant embedding method. It consists of two parts. In the first part, recent advances in the invariant embedding method as applied to transport calculations for gamma-ray are summarized. It includes a number of difficulties met in transport calculations for gamma-ray with real cross sections depending upon energy and angle, followed by the specific features of the invariant embedding method developed to overcome these difficulties. In the second part, some results of calculations for exposure buildup factors of gamma-ray from a point isotropic source in an infinite medium up to depth as large as 300 mean free paths by the invariant embedding method is described.

2. APPLICATION OF INVARIANT EMBEDDING METHOD TO TRANSPORT CALCULATIONS FOR GAMMA-RAY

2.1 DEFINITION OF FUNCTIONS AND BASIC EQUATIONS

Suppose we have a homogeneous slab of thickness X . The transmission function of the slab $T(E, \omega | E_0, \omega_0; X) dE d\omega$ is defined so that it represents the current of radiations transmitted through the slab with energy E in the range dE in the direction ω in the range $d\omega$ integrated over the exit surface of the slab due to an incident current of radiation with the unit intensity with energy E_0 in the direction ω_0 .

The angular variable ω represents the cosine of the polar angle between the direction of radiation and the axis perpendicular to the slab. The transmission function may alternatively be interpreted as representing the current density of transmitted radiations per unit area of the exit surface due to a plane parallel beam of incident radiations of the unit current density. The reflection function of the slab

$R(E, \omega|E_0, \omega_0; X)$ is defined in the same way as representing the current of radiations reflected by the slab.

In parts of the following description, we shall use the condensed expression $\mathbf{T}(X)$ and $\mathbf{R}(X)$ for the function $T(E, \omega|E_0, \omega_0; X)$ and $R(E, \omega|E_0, \omega_0; X)$. The matrices $\mathbf{T}(X)$ and $\mathbf{R}(X)$ of an infinite order are subscripted by the continuous variables E and ω .

The equation for the functions can be derived by considering how they change with the change of the slab thickness by an infinitesimal amount [1]. They are expressed as

$$\frac{d}{dX} \mathbf{R}(X) = \mathbf{R}(X) \dot{\mathbf{R}} \mathbf{R}(X) - \dot{\mathbf{T}} \mathbf{R}(X) - \mathbf{R}(X) \dot{\mathbf{T}} + \dot{\mathbf{R}} \quad (1)$$

$$\frac{d}{dX} \mathbf{T}(X) = [\mathbf{R}(X) \dot{\mathbf{R}} - \dot{\mathbf{T}}] \mathbf{T}(X) \quad (2)$$

where the functions $\dot{\mathbf{T}}$ and $\dot{\mathbf{R}}$ are independent of the slab thickness X given by

$$\dot{\mathbf{T}}(E, \omega|E_0, \omega_0) = \frac{\Sigma(E)}{\omega} \delta(E - E_0) \delta(\omega - \omega_0) - \frac{1}{\omega_0} \Sigma_s(E_0, \omega_0 \rightarrow E, \omega) \quad , \quad (3)$$

$$\dot{\mathbf{R}}(E, \omega|E_0, \omega_0) = \frac{1}{\omega_0} \Sigma_s(E_0, \omega_0 \rightarrow E, \omega) \quad (4)$$

where $\Sigma(E)$ is the macroscopic total cross section of the medium, $\Sigma_s(E_0, \omega_0 \rightarrow E, \omega)$, the macroscopic differential cross section for scattering from energy E_0 to E and from the direction ω_0 to ω and, $\delta(E)$, the Dirac delta function. Eqs.1 and 2 should be solved as the function of the slab thickness subject to the initial conditions

$$T(E, \omega|E_0, \omega_0; 0) = \delta(E - E_0) \delta(\omega - \omega_0) \quad (5)$$

$$R(E, \omega|E_0, \omega_0; 0) = 0 \quad (6)$$

As emphasized by Bellman [2] the numerical integration of these equations subject to the initial conditions (initial value problem) can generally be performed more easily than the numerical integration of the Boltzmann equation subject to the boundary conditions (boundary value problem). The direct numerical integration of these equations for thick slabs, however, still requires an excessive amount of computation times, because a very fine space mesh is required in actual calculations for gamma-ray.

2.2 APPLICATION OF INVARIANT EMBEDDING METHOD TO TRANSPORT PROBLEMS OF GAMMA-RAY

In this section, we discuss a number of difficulties met in transport calculations for gamma-ray with real cross sections depending upon energy and angle, followed by some specific feature of the invariant embedding method developed to overcome these difficulties.

1. Effect of Boundary

The angular distribution of radiations has a strong anisotropy at the boundary of slab. The intensity of

radiations with energy E below E_0 at the left boundary of the slab vanishes in the forward direction $0 \leq \omega \leq 1$ and has some finite value in the backward direction $-1 \leq \omega \leq 0$. On the other hand, the intensity of radiations at the right boundary of the slab vanishes in the backward direction radiation and has some finite value in the forward direction. It is impractical to expand such irregular distribution at the boundary in terms of the Legendre function $P_l(\omega)$ defined in the range $-1 \leq \omega \leq 1$, because the expansion converges very slowly. In fact, a dependable solution for gamma-ray albedo (reflection function) has never been provided by the discrete ordinate method based on the P_L approximation. According to the invariant embedding method, radiations in the forward directions represented by the transmission function $T(E, \omega | E_0, \omega_0; X)$ are treated separately from those in the backward direction represented by the reflection function $R(E, \omega | E_0, \omega_0; X)$. An expansion of the transmission function or the reflection function in terms of the Legendre function $P_l(\omega)$ defined in the range $0 \leq \omega \leq 1$ converges rather rapidly. Gamma-ray albedo were computed accurately by the method of invariant embedding with the order l between 7 to 15.

2. Anisotropy in the Scattering due to Energy-angle Correlation

Energy dependence of the gamma-ray cross sections $\Sigma(E)$ and $\Sigma_s(E_0, \omega_0 \rightarrow E, \omega)$ may well be treated with the multi-group approximation, since they varies with energy smoothly except for K or L edge. The energy range of interest is divided into a number of energy groups. Energy dependence of the cross sections are approximately represented by the multi-group cross sections defined by

$$\Sigma_n = \frac{1}{\Delta E_n} \int_n dE \Sigma(E) \quad (7)$$

$$\Sigma_{nm}(\omega, \omega_0) = \frac{1}{\Delta E_m} \int_m dE \int_n dE_0 \Sigma_s(E_0, \omega_0 \rightarrow E, \omega) \quad (8)$$

where $\int_n dE$ represents the integration over the group n and ΔE_m , the width of the group m respectively.

The differential scattering cross sections $\Sigma_s(E_0, \omega_0 \rightarrow E, \omega)$ vanishes for the energy $E > E_0$, since a photon is invariably scattered into lower energy. Therefore, the multi-group equation can be solved one by one from the highest energy group to the lower one. The problem can be reduced to solve the equation for the single energy group including the within-group scattering cross section $\Sigma_{nn}(\omega, \omega_0)$ (scattering from a group to the same group). It should be mentioned here that the within-group scattering cross section has a strong anisotropy due to energy- angle correlation in the scattering when the width of the energy group is very small compared with the maximum energy change in the scattering. The energy-angle correlation in the Compton scattering of photon is expressed as

$$\lambda - \lambda_0 = 1 - \cos \theta_s \quad (9)$$

where λ is the wave length after scattering in Compton wavelength unit and λ_0 , the wave length before

scattering and θ_s , the deflection angle. The deflection angle θ_s corresponding with within-group scattering in an energy group specified as $9.5\text{MeV} \leq E \leq 10.5\text{MeV}$ is limited by $1 - 0.00512 \leq \cos \theta_s \leq 1$, since the change in the wave $\lambda - \lambda_0$ is 0.00512 or less. The expansion of the within group scattering cross section for that energy group $\Sigma_{nm}(\omega, \omega_0)$ in terms of Legendre function $P_l(\omega)P_l(\omega_0)$ converges very slowly and requires many terms, since the scattering cross section behaves almost like the delta function $\delta(\omega - \omega_0)$. In our procedure, the microscopic double differential scattering cross section for Compton scattering is calculated using the analytical formula [1]

$$\sigma(\lambda_0, \omega_0 \rightarrow \lambda, \omega) = K(\lambda, \lambda_0) \text{Re} \frac{1}{\pi \sqrt{(1 - \omega_0^2 - \omega^2 - \gamma^2 + 2\gamma\omega\omega_0)}} \quad (\text{in Thomson unit}) \quad (10)$$

where

$$K(\lambda, \lambda_0) = \frac{3}{8} \frac{\lambda_0^2}{\lambda^2} \left[\frac{\lambda_0}{\lambda} + \frac{\lambda}{\lambda_0} + 2(\lambda_0 - \lambda) + (\lambda_0 - \lambda)^2 \right] \quad \text{for } \lambda_0 \leq \lambda \leq \lambda_0 + 2$$

$$= 0 \quad \text{otherwise} \quad (11)$$

and

$$\gamma = 1 + \lambda_0 - \lambda \quad (12)$$

Based on the formula 10, the integration with respect to λ is performed analytically and the integration with respect to λ_0 numerically in calculating the multi-group cross sections $\Sigma_{nm}(\omega, \omega_0)$.

Kistos et al. [3] reported that an extremely fine angular mesh was required in their calculations of gamma-ray buildup factors by the SN1D code, that is presumed to be based on the expansion of the within-group scattering cross sections in terms of Legendre function $P_l(\omega)P_l(\omega_0)$. The error due to angular mesh was estimated 2% at depth of 30 mean free paths, when S_{64} Gaussian quadrature was applied. Based on our procedure, the error in gamma-ray buildup factor calculations due to angular mesh is estimate 2% or less at depths of 30 mfp and 10% or less at depths of 100 mfp, when S_{13} Gaussian quadrature in the range $0 \leq \omega \leq 1.0$ was applied [4].

3. Influence of the Space Mesh

The energy dependence of the cross section gives rise to another difficulty, an excessive amount of space meshes, to be overcome in the transport calculations for gamma-ray. The attenuation rate per unit thickness for radiations moving in the direction ω with energy E is given by the factor $\Sigma(E)/\omega$. In order to solve numerically the differential equation with respect to the space variable including such attenuation factor, the space mesh width ΔX should approximately be chosen to satisfy the condition $\Delta X \Sigma(E)/\omega \leq 1$. In terms of the mean free path of gamma-ray with the source energy E_0 , the required space mesh width is

approximately given as

$$\Delta X \leq \omega \Sigma(E_0) / \Sigma(E) \quad \text{mean free paths for the source energy } E_0 \quad (13)$$

For example, a space mesh width required in transport calculations of gamma-ray in a medium of lead with energy 0.2 MeV from the source radiations with 1.0 MeV in the direction given as the smallest value of ω based on S_{13} Gaussian quadrature in the range $0 \leq \omega \leq 1.0$ should be less than $0.00922 \times 0.0684 / 0.943 \approx 1/1500$ mfp. It is too small to extend transport calculations beyond depths of 40 mfp.

1) Method of Solution for Reflection Function

The equation for the reflection function for a semi-infinite medium $\mathbf{R}(\infty)$ can be derived from Eq.1 based on the fact that the differential term $d/dX \mathbf{R}(X)$ vanishes, since the reflection function for a semi-infinite medium is invariant with respect to the addition to the boundary of a layer of the same composition. The equation is expressed as

$$\mathbf{R}(\infty) \dot{\mathbf{R}} \mathbf{R}(\infty) - \dot{\mathbf{T}} \mathbf{R}(\infty) - \mathbf{R}(\infty) \dot{\mathbf{T}} + \dot{\mathbf{R}} = 0 \quad (14)$$

The equation is free from the space variable and can be solved efficiently by the iteration method developed by the author [1]. Recently, gamma-ray albedo data (reflection function) was generated for various materials by the invariant embedding method by Kadotani and the author [5]. It was shown that number albedos obtained by the invariant embedding method agree very well with Monte Carlo calculations using MCNP within the discrepancy less than 1%. The calculation of the differential albedos (the reflection function) can efficiently be performed by the invariant embedding method. It takes about 30 sec. by using a personal computer with 500MHz processor to compute all the elements of $\mathbf{R}(\infty)$ based on 50 energy groups and 13 angular divisions.

The reflection function for a slab of finite thickness $\mathbf{R}(X)$ can only be obtained by solving Eq.1 with a very fine mesh described previously. The function $\mathbf{R}(X)$, however, approaches $\mathbf{R}(\infty)$ rapidly, when the thickness of the slab is extended up to a few mean free paths.

2) Method of Solution for Transmission Function

The method of solution for the transmission function has been developed to overcome the difficulty of the excessive amount of spatial meshes by the author [1,6]. He introduced the modified transmission function $\tilde{\mathbf{T}}(X)$, that is defined physically as the current of transmitted radiations due to a current of the unit intensity from a source in an arrangement where a semi-infinite medium of the same composition as the slab is placed behind the source as illustrated in Fig.1.

The equation for the modified transmission function is expressed as

$$\frac{d}{dX} \tilde{\mathbf{T}}(E, \omega | E_0, \omega_0; X) = -\frac{\Sigma(E)}{\omega} \tilde{\mathbf{T}}(E, \omega | E_0, \omega_0; X) + \int_0^{E_0} dE' \int_0^1 d\omega' C(E, \omega | E', \omega') \tilde{\mathbf{T}}(E', \omega' | E_0, \omega_0; X) \quad (15)$$

where

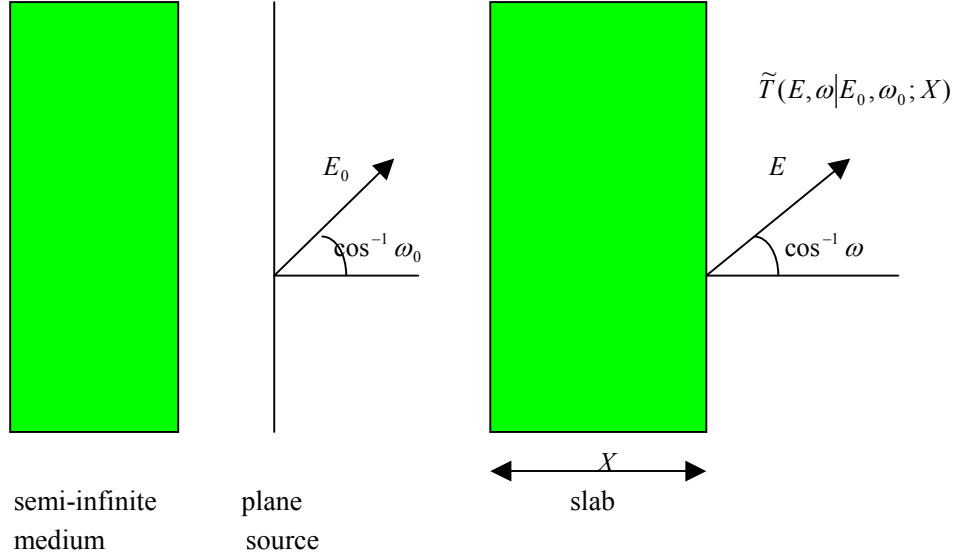


Figure 1. Modified transmission function

$$C(E, \omega | E_0, \omega_0) = \frac{1}{\omega_0} \Sigma_s(E_0, \omega_0 \rightarrow E, \omega) + \frac{1}{\omega_0} \int_0^{E_0} dE' \int_0^1 d\omega' R(E, \omega | E', \omega'; \infty) \Sigma_s(E_0, \omega_0 \rightarrow E', -\omega') \quad (16)$$

Eq.15 can be derived by replacing $\mathbf{R}(X)$ with $\mathbf{R}(\infty)$ in Eq.2. The function $C(E, \omega | E_0, \omega_0)$ is independent of the space variable, representing the effective forward scattering. The first term on the right-hand side of Eq.16 represents the radiations scattered directly in the forward direction and the second term those scattered first in the backward direction and then reflected in the forward direction by the medium behind the front surface. The reflection function behind the front surface is invariably given by $\mathbf{R}(\infty)$ due to the semi-infinite medium behind the slab. The initial condition of the modified transmission is given as

$$\tilde{T}(E, \omega | E_0, \omega_0; 0) = \delta(E - E_0) \delta(\omega - \omega_0) \quad (17)$$

It can be proved that the modified transmission function satisfies the functional relation

$$\tilde{T}(X + X') = \tilde{T}(X') \tilde{T}(X) \quad (18)$$

It can further be proved that there is a relation between the modified transmission function and the ordinary transmission function expressed as

$$\mathbf{T}(X) = \tilde{\mathbf{T}}(X) [\mathbf{E} - \mathbf{R}(\infty) \mathbf{R}(X)] \quad (19)$$

where \mathbf{E} represents the unit matrix. When the thickness X is greater than a few mean free paths, Eq.19 can approximately reduced to

$$\mathbf{T}(X) = \tilde{\mathbf{T}}(X)[\mathbf{E} - \mathbf{R}(\infty)^2] \quad (20)$$

Eq.15 is classified mathematically as the first order linear system with constant coefficients in the ordinary differential equations. It can be solved much more easily than Eq.2 that is classified as the first order linear system with coefficients depending on the spatial variable X .

Based on the multi-group approximation with respect to energy and the discrete ordinates approximation with respect to the angular variable, Eq.15 is reduced to

$$\frac{d}{dX} \mathbf{y}^{(n)}(X) = \mathbf{A}^{(n)} \mathbf{y}^{(n)}(X) + \mathbf{b}^{(n)}(X) \quad n=m, m+1, \dots, N \quad (21)$$

Here, we divide the energy range of interest into N groups and the range of the angular variable $0 \leq \omega \leq 1$ into G sub-regions such as $\{\bar{\omega}_{k-1} \leq \omega \leq \bar{\omega}_k; k=1,2,\dots,G\}$, where $\bar{\omega}_{k-1}$ and $\bar{\omega}_k$ are the boundary values of the sub-region k and $\bar{\omega}_0 = 0$ and $\bar{\omega}_G = 1$. $\mathbf{y}^{(n)}(X)$ in Eq.21 is the column vector of the dimension G , the element of which is given by

$$y_i^{(n)}(X) = \tilde{T}_{nm}(\omega_i, \omega_j; X) \quad i = 1, 2, \dots, G \quad (22)$$

$\tilde{T}_{nm}(\omega_i, \omega_j; X)$ represents the modified transmission function from the group m to n and from the angular division ω_j , the mid value of ω in the sub-region j , to ω_i defined by

$$\tilde{T}_{nm}(\omega_i, \omega_j; X) = \frac{1}{\Delta E_m} \int_n dE \int_m dE_0 \tilde{T}(E, \omega_i | E_0, \omega_j; X) \quad (23)$$

$\mathbf{A}^{(n)}$ is the matrix of the dimension G , the element of which is given by

$$a_{ij}^{(n)} = -\frac{\sum_n \delta_{ij} + w_j C_{nm}(\omega_i, j)}{\omega_i} \quad (24)$$

where

$$C_{nm}(\omega_i, j) = \frac{1}{\Delta E_m w_j} \int_n dE \int_m dE_0 \int_{\omega_j}^{\omega_i^+} d\omega C(E, \omega_i | E_0, \omega), \quad (25)$$

and w_j , the width of the angular sub-region j , and δ_{ij} , the Kronecker delta. The function $\mathbf{b}^{(n)}(X)$ is the column vector of the dimension G , the element of which is given by

$$b_i^{(n)}(X) = \sum_{l=m}^{n-1} \sum_{k=1}^G w_k C_{nl}(\omega_i, k) \tilde{T}_{lm}(\omega_k, \omega_j; X) \quad (26)$$

Eq.21 should be solved subject to the initial condition

$$\tilde{T}_{nm}(\omega_i, \omega_j; 0) = \frac{1}{w_i} \delta_{nm} \delta_{ij}. \quad (27)$$

Two kinds of method have been developed by the author to solve Eq.21 subject to the initial condition in Eq.27.

- (1) the angular eigenvalue method [6].
- (2) The method of direct numerical integration [1].

According to the angular eigenvalue method, Eq.21 is solved analytically with respect to the slab thickness X . The solutions are expressed in terms of a linear combination of the exponential functions

$\{\exp(\lambda_{ni}X) : n = m - N, i = 1 - G\}$, where the constants $\{\lambda_{ni}; i = 1 - G\}$, called the angular eigenvalue, are determined as the eigenvalues of the matrix $\mathbf{A}^{(n)}$. The solutions are, therefore, free from the space mesh width.

According to the direct numerical integration method, Eq.21 is integrated numerically with respect to the slab thickness X by using the Runge-Kutta method for the first step. The solutions for extended thickness are obtained by using the functional relation equivalent with Eq.18

$$\tilde{T}_{nm}(\omega_i, \omega_j; X + X') = \sum_{l=m}^n \sum_{k=1}^G w_k \tilde{T}_{nl}(\omega_i, \omega_k; X') \tilde{T}_{lm}(\omega_k, \omega_j; X). \quad (28)$$

Since the solution for the slab thickness doubled can be obtained successively by using the functional relation in Eq.28, calculations can be extended to a large depth without difficulty starting from a very fine mesh for the first step.

The influence of the space mesh upon transport calculations for gamma-ray is checked by comparing between the solutions obtained by the direct numerical integration method (NI method) and those obtained by the angular eigenvalue method (AE method). Although the latter solution is given analytically with respect to the depth, it may have a rounding off error when an angular eigenvalue happens to be very close to other one, since it is assumed in deriving analytical solutions that the angular eigenvalues differ with each other. The result of comparisons for gamma-ray exposure buildup factors for a point isotropic source with energy 1.0 MeV in the infinite medium of lead is shown in Table 1. The buildup factors are computed up to depths of 100 mfp both by NI method and AE method based on 50 energy groups and 15 angular divisions. Buildup factors for a plane isotropic source computed are transformed to buildup factors for the corresponding point isotropic source by using the conversion formula (30) given in the next section. The difference between solutions by both methods decreases rapidly with the mesh width used in the integration by Runge-Kutta method for the first step in NI method. The difference is 0.02% or less up to depth of 100 mfp, when the mesh width of 1/1024 mfp is used. The same results were obtained for other materials including water and iron at typical source energies of 10 MeV, 1.0 MeV and 0.1 MeV. The error due to space mesh in the present method is confirmed to be 0.03% or less up to depth 100 mfp, when the initial mesh width of 1/512 mfp or 1/1024 mfp is used. These results indicate both NI method and AE method provide quite accurate solutions up to depth as large as 100 mfp. It is proved that the invariant embedding method using the modified transmission function is practically free from the difficulty concerning the space mesh, and can be applied to the deep penetration problems.

Table 2. Influence of space mesh upon gamma-ray exposure buildup factor calculation
Lead, source energy 1.0 MeV

Depth/ Δ	BF(numerical) [*] /BF(analytical) ^{**}					
	1/64 mfp	1/128 mfp	1/256 mfp	1/512 mfp	1/1024 mfp	1/2048mfp
1.0 mfp	1.1921	1.0514	1.0093	1.0010	1.0001	1.0000
10.0	1.3190	1.0801	1.0130	1.0013	1.0001	1.0000
40.0	1.3373	1.0831	1.0132	1.0013	1.0001	1.0000
70.0	1.3387	1.0833	1.0132	1.0014	1.0002	1.0001
100.0	1.3393	1.0834	1.0132	1.0014	1.0001	1.0001

* buildup factor obtained by the direct numerical integration method using Runge-Kutta method with initial mesh width Δ .

** buildup factor obtained analytically by the angular eigenvalue method

It was confirmed recently that the invariant embedding method with 50 to 80 energy groups and 13 angular divisions in the range $0 \leq \omega \leq 1$ is able to provide buildup factors of gamma-ray from a point isotropic source in an infinite medium with a negligible error due to space mesh (usually less than 0.03%) and an error about 10% or less due to the multi-group and discrete ordinate approximations up to depths of 100 mfp. [4]

4. Buildup Factor for Point Isotropic Source

Since the buildup factors for point isotropic sources in infinite homogeneous media are currently used in shielding calculations for gamma-ray, a method to transform a buildup factor for a plane isotropic source to the buildup factor for the corresponding point isotropic source has been developed [4,6]. We define the energy-dependent buildup factor for a point isotropic source in an infinite homogeneous medium

$B^{pi}(E, X)$ by the equation

$$\phi^{pi}(E, X) = B^{pi}(E, X) \exp(-\Sigma(E_0)X) / (4\pi X^2) \quad (29)$$

where $\phi^{pi}(E, X)$ represents the flux density of gamma-ray with energy E at the distance of X from the point isotropic source with energy E_0 . Based on the fact that the plane source is an assemble of the point isotropic sources distributed uniformly on the plane, we get the equation

$$B^{pi}(E, X) = -2X \exp(\Sigma(E_0)X) \frac{d}{dX} \phi^{pi}(E, X) \quad (30)$$

where $\phi^{pi}(E, X)$ represents the flux density due to the corresponding plane isotropic source in the infinite medium. The flux $\phi^{pi}(E, X)$ can be obtained from the modified transmission function and the reflection function for the semi-infinite medium. Eq.30 includes the derivative of $\phi^{pi}(E, X)$ with respect to X , that can be performed analytically for the solution obtained by the angular eigenvalue method. The desired derivative for the solution obtained by the direct numerical integration method can be computed by using Eq.21 where it is given by the right hand side of the equation.

3. BUILDUP FACTORS OF GAMMA-RAY FOR VERY DEEP PENETRATION

Some shielding calculations for a postulated severe accident of a nuclear power station requires the gamma-ray buildup factors beyond depth of 100 mfp. For example, a concrete wall postulated in a shielding calculation has an accumulated thickness of 20 m, that is equivalent with 375 mean free paths or more for gamma-ray with energy 0.5 MeV or less that is dominant in the accident. Calculations of gamma-ray buildup factor for depths as large as 300 mfp are challenged by the method of invariant embedding. As described previously, the angular eigenvalue method can be applied to very deep penetration, since solutions are given analytically with respect to slab thickness. The direct numerical integration method is also applicable to very deep penetration problems. Once the modified transmission function $\tilde{T}(X_0)$ for a typical slab thickness X_0 is obtained, the transmitted current for extended

thickness can be computed successively by using the equation

$$\mathbf{J}_i((n+1)X_0) = \tilde{\mathbf{T}}(X_0)\mathbf{J}_i(nX_0) \quad (31)$$

where the column vector $\mathbf{J}_i(X)$ represents the transmitted current density through the slab of thickness

X in the arrangement illustrated in Fig 1. Eq.31 includes the product of a matrix with a vector, that can be performed much more efficiently than computations by Eq.28 including the product of a matrix with a matrix. The exposure buildup factors for gamma-ray from point isotropic sources in infinite media are computed up to depths of 300 mfp by the invariant embedding for some materials including concrete, water, iron and air. The exposure buildup factors for concrete and iron at typical source energies of 450keV, 150keV and 100keV are given in Table 3. Most computations are performed with 95 energy groups and 15 angular divisions based on Gaussian quadrature in the range $0 \leq \omega \leq 1$.

The influence of angular mesh and energy mesh upon buildup factors are analyzed based on the method of error analysis developed recently by the author. [4] We shall denote a buildup factor computed with a total number of angular divisions G and a total number of energy groups N at a depth of X by $B(G, N; X)$. It was found through the survey calculations for gamma-ray that the buildup factor ratios

$\{B(G, N, X) / B(15, N, X); G = 7 - 13\}$ changes with N by a negligible amount (0.2% or less) when $G \geq 7$

and $N \geq 40$. It was also found that the buildup factor ratios $\{B(G, N; X) / B(15, N; X); G = 7 - 13\}$ are smaller than unity, and approach unity when the number of angular divisions G increases. We introduce an angular error coefficient defined by

$$Ea(G, X) = B(G, N; X) / B(\infty, N; X) \quad (32)$$

where $B(\infty, N; X)$ represents the exact value of buildup factor to be obtained if G could be extended to infinite. The angular error coefficient is independent of the number of energy groups N under the condition described previously. Although we can not obtain the exact value of the angular error coefficient, we can calculate the limiting angular error coefficient $\bar{E}a(G, X)$ that satisfies the condition

$$\bar{E}a(G, X) \leq Ea(G, X) \quad (33)$$

from the buildup factor ratios $\{B(G, N; X) / B(15, N; X); G = 5 \sim 13\}$, based on the fact that these ratios are smaller than unity and approach unity with G increasing. Similarly, the energy error coefficient is defined as

$$Ee(N, X) = B(G, N; X) / B(G, \infty; X) \quad (34)$$

We can compute the limiting energy error coefficients $\bar{E}e(G, X)$ satisfying the condition

$$Ee(N, X) \leq \bar{E}e(G, X) \quad (35)$$

Table 3. Gamma-ray exposure buildup factors for point isotropic sources¹

Material	Concrete			Iron			
	Source Energy	450keV	150 keV	100 keV	450keV	150 keV	100 keV
Depth(mfp)							
1.0	2.32E+00	2.81E+00	2.77E+00	2.00E+00	1.67E+00	1.39E+00	
5.0	1.28E+01 ²	1.50E+01	1.12E+01	7.64E+00	3.38E+00	2.07E+00	
10.0	3.92E+01	4.29E+01	2.57E+01	1.88E+01	5.12E+00	2.60E+00	
15.0	8.29E+01	8.82E+01	4.50E+01	3.43E+01	6.65E+00	3.00E+00	
20.0	1.45E+02	1.54E+02	6.91E+01	5.39E+01	8.06E+00	3.32E+00	
30.0	3.32E+02	3.57E+02	1.31E+02	1.05E+02	1.06E+01	3.84E+00	
40.0	6.04E+02	6.72E+02	2.11E+02	1.71E+02	1.29E+01	4.26E+00	
50.0	9.65E+02	1.12E+03	3.09E+02	2.52E+02	1.51E+01	4.61E+00	
60.0	1.42E+03	1.70E+03	4.24E+02	3.47E+02	1.71E+01	4.93E+00	
70.0	1.97E+03	2.45E+03	5.56E+02	4.55E+02	1.91E+01	5.21E+00	
80.0	2.61E+03	3.37E+03	7.06E+02	5.77E+02	2.10E+01	5.48E+00	
90.0	3.35E+03	4.49E+03	8.73E+02	7.12E+02	2.29E+01	5.72E+00	
100.0	4.19E+03	5.80E+03	1.06E+03	8.60E+02	2.47E+01	5.95E+00	
110.0	5.13E+03	7.34E+03	1.26E+03	1.02E+03	2.65E+01	6.17E+00	
120.0	6.18E+03	9.11E+03	1.48E+03	1.20E+03	2.83E+01	6.38E+00	
130.0	7.33E+03	1.11E+04	1.72E+03	1.38E+03	3.01E+01	6.58E+00	
140.0	8.59E+03	1.34E+04	1.98E+03	1.58E+03	3.19E+01	6.77E+00	
150.0	9.95E+03	1.60E+04	2.26E+03	1.79E+03	3.36E+01	6.96E+00	
160.0	1.14E+04	1.88E+04	2.56E+03	2.02E+03	3.54E+01	7.13E+00	
170.0	1.30E+04	2.20E+04	2.88E+03	2.26E+03	3.72E+01	7.29E+00	
180.0	1.47E+04	2.55E+04	3.23E+03	2.51E+03	3.89E+01	7.44E+00	
190.0	1.65E+04	2.94E+04	3.59E+03	2.77E+03	4.06E+01	7.58E+00	
200.0	1.85E+04	3.36E+04	3.98E+03	3.04E+03	4.23E+01	7.70E+00	
210.0	2.05E+04	3.82E+04	4.39E+03	3.33E+03	4.40E+01	7.82E+00	
220.0	2.27E+04	4.32E+04	4.83E+03	3.62E+03	4.57E+01	7.93E+00	
230.0	2.50E+04	4.86E+04	5.30E+03	3.93E+03	4.73E+01	8.02E+00	
240.0	2.74E+04	5.45E+04	5.78E+03	4.25E+03	4.90E+01	8.10E+00	
250.0	2.99E+04	6.09E+04	6.30E+03	4.59E+03	5.06E+01	8.18E+00	
260.0	3.26E+04	6.77E+04	6.84E+03	4.93E+03	5.22E+01	8.24E+00	
270.0	3.53E+04	7.51E+04	7.42E+03	5.28E+03	5.37E+01	8.29E+00	
280.0	3.82E+04	8.30E+04	8.02E+03	5.64E+03	5.52E+01	8.33E+00	
290.0	4.13E+04	9.14E+04	8.65E+03	6.02E+03	5.67E+01	8.37E+00	
300.0	4.44E+04	1.01E+05	9.32E+03	6.40E+03	5.82E+01	8.39E+00	

¹ Computed by IE method with 95 energy groups and 15 angular divisions

² Read as 1.28x10¹

from the buildup factor ratios $\{B(G, N; X) / B(G, 95; X); N = 50 - 95\}$, based on the fact confirmed by actual calculations that these buildup factor ratios are larger than unity and approach unity with N increasing. The limiting angular error coefficients and the limiting energy error coefficients obtained are given in Tables 4 and 5 respectively. It is shown that the error in the buildup factors due to energy and angular meshes amounts to about 30 – 85% at depths of 300 mfp, although it is less than 10% at depths of 100 mfp. The error of this magnitude is acceptable in shielding calculations, since the intensity of the primary radiations transmitted thorough the medium without suffering any collision are reduced by the factor $\exp(-300) \approx 10^{-130}$ before reaching depths of 300 mfp.

Table 4. Limiting angular error coefficient for buildup factors¹

The total number of angular division is 15

Material	Concrete			Iron		
E ₀	450keV	150 keV	100 keV	450keV	150 keV	100 keV
Depth(mfp)						
10.0	0.996	0.998	0.998	0.995	0.998	0.999
20.0	0.991	0.994	0.995	0.990	0.995	0.997
40.0	0.981	0.987	0.989	0.980	0.990	0.995
60.0	0.971	0.980	0.983	0.971	0.985	0.992
100.0	0.950	0.965	0.971	0.951	0.972	0.980
150.0	0.919	0.942	0.948	0.914	0.915	0.906
200.0	0.867	0.908	0.906	0.849	0.805	0.769
250.0	0.790	0.858	0.845	0.759	0.675	0.620
300.0	0.699	0.794	0.769	0.657	0.549	0.488

¹ [Computed buildup factor]/[The correct buildup factor] > The coefficient in this table

Table 4. Limiting energy error coefficient for buildup factors¹

The total number of energy groups is 95

Material	Concrete			Iron		
E ₀	450keV	150 keV	100 keV	450keV	150 keV	100 keV
Depth(mfp)						
10.0	1.000	1.000	1.000	1.001	1.001	1.001
20.0	1.000	1.000	1.000	1.003	1.004	1.003
40.0	1.010	1.010	1.010	1.009	1.016	1.011
60.0	1.010	1.010	1.020	1.018	1.031	1.025
100.0	1.030	1.040	1.070	1.046	1.088	1.068
150.0	1.070	1.090	1.160	1.102	1.197	1.157
200.0	1.130	1.170	1.290	1.182	1.355	1.286
250.0	1.210	1.270	1.470	1.293	1.570	1.465
300.0	1.310	1.390	1.710	1.438	1.853	1.708

¹ [Computed buildup factor]/[The correct buildup factor] < The coefficient in this table

CONCLUSION

Recent advances in the invariant embedding method as applied to transport calculations for gamma-ray with real cross sections are summarized. It was proved through actual calculations that the invariant embedding method has the features: 1) the method can well treat with the strong anisotropy in the angular distribution of radiations at the boundary of slab, 2) the strong anisotropy in within-group scattering cross section for gamma-ray due to the energy-angle correlation in the scattering is overcome by using the analytical formula for the double differential cross section, 3) the method is proved to be practically free from space mesh and can be applied to deep penetration problems. Some results of calculations for exposure buildup factors of gamma-ray from a point isotropic source in an infinite medium up to depths as large as 300 mean free paths are presented together with the coefficient representing limiting value of error.

ACKNOWLEDGEMENTS

The author thanks Mr. T. Tuchida of Kyoto university for his contribution to the calculations of buildup factors up to depths of 300 mfp.

REFERENCES

1. A. Shimizu, K. Aoki, *Application of Invariant Embedding to Reactor Physics*, Academic Press, (1972).
2. R. Bellman, R. Kalaba, *Proc. Nat. Acad. Sci. USA*, **42**, 629 (1956).
3. A. Kitsos, *et al.*, "Determination of point isotropic buildup factors of gamma rays including incoherent and coherent scattering for aluminum, iron, lead, and water by the discrete ordinate method", *Nucl. Sci. Engng.*, **117**, 49 (1994).
4. A. Shimizu, "Calculation of gamma-ray buildup factors up to depths of 100 mfp by the method of invariant embedding", *J. Nucl. Sci. Technol.*, **39**, 477-486 (2002).
5. H. Kadotani, A. Shimizu, "Gamma ray albedo data generated by the invariant embedding method", *J. Nucl. Sci. Technol.*, **35**, 584-594 (1998).
6. A. Shimizu, "Development of angular eigenvalue method for radiation transport problems in slabs and its application to penetration of gamma rays", *J. Nucl. Sci. Technol.*, **37**, 15-25 (2000).